View metadata, citation and similar papers at core.ac.uk
brought to you by CORE
provided by JAMSTEC Repository

Lithium and strontium isotopic systematics of waters around Ontake volcano, Japan: Implications for deep-seated fluids and earthquake swarms

Yoshiro Nishio[1*], Kei Okamura[2], Masaharu Tanimizu[1], Tsuyoshi Ishikawa[1], Yuji Sano[3]

[1] Kochi Institute for Core Sample Research, Japan Agency for Marine-Earth Science and Technology (JAMSTEC), Monobe B200, Nankoku, Kochi 783-8502, Japan

[2] Center for Advanced Marine Core Research, Kochi University, Monobe B200, Nankoku, Kochi 783-8502, Japan

[3] Ocean Research Institute, University of Tokyo, Minamidai 1-15-1, Nakano, Tokyo 164-8639, Japan

Manuscript submitted to *Earth and Planetary Science Letters*

Manuscript revised, July 1, 2010

(8570 words in main text, 3 table and 7 figures)

Corresponding author (Yoshiro Nishio)

E-mail: nishio@jamstec.go.jp; Tel: +81-46-867-9354; Fax: +81-46-867-9315

Keywords:

lithium isotope; strontium isotope; earthquake swarm; spring; deep-seated fluid; lower crust

Abstract

Since 1976, earthquake swarms have occurred beneath the southeast flank of Ontake volcano in central Japan. Electrical conductivity surveys have shown that these earthquake swarms are associated with the upwelling of deep-seated fluid. To investigate the nature of the deep-seated fluid, we analyzed $^{7}Li/^{6}Li$ and $^{87}Sr/^{86}Sr$ ratios of water samples collected from springs and wells around Ontake volcano in 2000, 2003, 2005, 2007, and 2009. The Li and Sr isotopic compositions of these water samples are largely explained by binary component mixing between near-surface meteoric water and non-surface fluid at each sampling site. On the basis of their Cl/Li and Cl/Sr ratios, we singled out water samples whose Li and Sr isotopic ratios were minimally affected by meteoric water contamination to represent non-surface fluids. The Li and Sr isotopic compositions of most Ontake non-surface fluids, except for samples from the earthquake swarm region, can be explained as the result of volcanic fluids reacting with basement rocks, where they acquired upper crustal signatures. We attribute the fluid associated with the region of earthquake swarms to the lower crust beneath the study area.

1. INTRODUCTION

Knowledge of the nature and origin of fluids in the deep crust is crucial for understanding the geochemical evolution of the Earth. Fluids in the deep crust also play an important role in the occurrence of intraplate earthquakes (IIO et al., 2002). The M6.8 western Nagano Prefecture earthquake occurred in September 1984 beneath the southeast flank of Ontake volcano in central Japan (Fig. 1a). Earthquake swarm activity in the region began in August 1976 (Fig. 1a). Since the first historic eruption of Ontake volcano in October 1979, earthquake swarms have occurred continuously. Events greater than M4 occur once or twice a year. As shown in Figs. 1b and 1c, electrical conductivity surveys have revealed a low-resistivity fluid conduit from at least 10 km depth to the surface beneath the earthquake swarm region (KASAYA et al., 2002; KASAYA and OSHIMAN, 2004). The event hypocenters are distributed around the edge of this conduit (KASAYA et al., 2002). In the earthquake swarm region, ground uplift of 3–6 mm was detected during a period from 2002 to 2004 (KIMATA et al., 2004). The point pressure source causing the uplift is at a depth of about 2–3 km, and the estimated volume increase from 2002 to 2004 is 5×10^5 m^3 (KIMATA et al., 2004). It has been proposed that ascending deep-seated fluid causes the crustal deformation in the southeast flank

of Ontake volcano (KASAYA et al., 2002; KASAYA and OSHIMAN, 2004; KIMATA et al., 2004). The origin of this fluid is still unknown.

It is difficult to research deep-seated fluids from spring and well water samples using traditional hydrogen and oxygen isotopic compositions owing to contamination from near-surface meteoric water. Lithium is relatively unsusceptible to contamination from meteoric water because the Li content of deep-seated fluid is significantly higher than that of near-surface water. The amount of Li leached from rock to fluid increases dramatically with temperature, and the leached Li is retained in the fluid as it cools (YOU et al., 1996; JAMES et al., 2003). Approximately 70% of Li contained initially in fresh basalt leaches into the aqueous phase at 400 ˚C, when fluid/rock mass ratios are near unity (SEYFRIED et al., 1984). Lithium has two stable isotopes, ^{7}Li and ^{6}Li, with respective relative abundances of 92.5% and 7.5%, and ^{7}Li/^{6}Li ratios may provide further insight into the origin of deep-seated fluids. Because Li is present only in the +1 valence, its isotopic composition is not influenced by redox reactions. Also, Li is not a nutrient and does not participate in biologically mediated reactions. These characteristics make Li isotopes a promising tool for researching the origin of spring and well waters. We therefore analyzed ^{7}Li/^{6}Li ratios together with ^{87}Sr/^{86}Sr ratios and chemical compositions of

67 spring and well waters to investigate the crustal fluid regime beneath Ontake volcano.

68 Documented Li isotopic data on spring waters are scarce (TOMASCAK et al., 2003;
69 MILLOT et al., 2007) because accurate Li isotopic measurement was difficult before Tomascak
70 et al. (1999) adapted a multi-collector inductively coupled plasma mass spectrometer
71 (MC-ICP-MS) technique.

72

73 **2. GEOLOGICAL SETTING AND PREVIOUS GEOCHEMICAL RESULTS**

74 Mount Ontake is an isolated stratovolcano (3063 m) in central Japan (35˚54′N,
75 137˚29′E). Beneath the region are two subducting slabs: the Philippine Sea plate at a depth of 70
76 km subducting from the southeast overlaps with the older Pacific plate at a depth of 240 km
77 subducting from the east (KIMURA and YOSHIDA, 1999; NAKAJIMA and HASEGAWA, 2007).
78 The thickness of the crust in this region ranges from 30 to 35 km, and the lower boundary of the
79 seismic upper crust is at 16 km depth (ZHAO et al., 1992; IIDAKA et al., 2003). Interpolating
80 from the depth of the seismic zone, it has been estimated that the temperature at 6 km depth is
81 about 250 ˚C (TANAKA and ITO, 2002).

82 As shown in Fig. 1a, Ontake volcano is underlain by a Cretaceous–Paleogene caldera

83 complex consisting of the Nohi rhyolite and younger granitoids and by a Mesozoic melange
84 complex of the Mino belt (GEOLOGICAL SURVEY OF JAPAN, 1995). The Mino belt in this region
85 (Misogawa complex) consists of two lithologic units, one dominantly sandstone and the other
86 composed of pelagic chert and hemipelagic siliceous mudstone (SHUTO and OTSUKA, 2004). At
87 Ontake, volcanic activity began in middle Pleistocene time, and its volcanic products are mostly
88 lavas and pyroclastics of andesitic composition plus minor amounts of rhyolite, dacite, and
89 basalt.

90 Since its first historic eruption of October 1979, Ontake volcano has erupted in May
91 1991 and in March 2007. The Ontake area has many springs from which CO_2-enriched gases
92 emanate (Fig. 1a). Periodic geochemical surveys of these spring gases since November 1981
93 have shown that their $^3He/^4He$ ratios decrease with distance from the volcano (SANO et al.,
94 1984; SANO et al., 1998; TAKAHATA et al., 2003). It has been inferred that volcanic helium with
95 high $^3He/^4He$ passed through the basement rocks, where they picked up upper-crustal helium
96 with low $^3He/^4He$ (SANO et al., 1984; SANO et al., 1998; TAKAHATA et al., 2003).

97

98 **3. SAMPLING AND ANALYTICAL PROCEDURES**

3.1. Sampling Procedures and Chemical Compositions

Fluid samples analyzed in this study were collected in June 2000, June 2003, June 2005, June 2007, and July 2009 (Table 1). Most water samples were from natural flow springs and natural flow wells where CO_2-enriched gases were bubbling up from the bottom of pools (SANO et al., 1998; TAKAHATA et al., 2003), whereas water samples from sites KKH-B, KNS-C, KYK, KRB, and NGG-B were pumped up (Table 1; site locations in Fig. 1a). Samples from sites SRK and SJM may be contaminated with river water, because the gases were bubbling up in pools located near riverbank. Site AKG is also located at the edge of a river, and its sample may represent river water rather than spring water.

The samples were passed through a 0.2 μm PTFE syringe filter at the sampling site. Subsequent procedures such as column separation were undertaken under filtered airflow (cleanliness level better than class 1000) and using 18.2 MΩ–grade water prepared by a Millipore purification system. The clean laboratory and all analytical equipment used in this study were at Kochi core center. To prevent precipitation during storage, ultrapure HNO_3 (Kanto Chemical Co.) was added to sample solutions. Concentrations of Si were determined with an inductively coupled plasma atomic emission spectrograph (Optima 4300DV CYCRON,

PerkinElmer) using 100 times diluted sample solutions, and concentrations of K, Ca, Mg, Na, and Cl were determined with an ion chromatograph (ICS-2000, Dionex) using 100 times diluted sample solutions. An absolute calibration curve method was used to determine these concentrations. Concentrations of Li, Rb, and Sr were determined with a quadrupole inductively coupled plasma mass spectrometer (ELAN-DRC II, PerkinElmer) using 360 times diluted sample solutions containing an internal standard of indium. Uncertainties for all these measurements are better than ±3%, as estimated from the reproducibility (2RSD) of standard solutions whose salt contents are higher than analyzed samples.

3.2. Li and Sr Isotopic Measurements

3.2.1. Column Separation

Li and Sr isotope ratios were measured with a multi-collector inductively coupled plasma mass spectrometer (MC-ICP-MS) (Neptune, Thermo Sci. Co.) and a thermal ionization mass spectrometer (TIMS) (Triton, Thermo Sci. Co.), respectively, after two-step column separation. Most analytical protocols followed procedures documented previously (NISHIO and NAKAI, 2002; NISHIO et al., 2004), which modified that of Tomascak et al. (1999). Because the

131 Neptune MC-ICP-MS used in this study was able to determine Li isotopic ratio more precisely
132 than the Isoprobe MC-ICP-MS used in previous studies, we adopted additional Li purification
133 (two-step column separation) following procedures of Jeffcoate et al. (2004).

134 The first-stage separation was carried out using a quartz glass column filled to a
135 height of 6 cm with a 6 ml Bio-Rad AG50W X8 (200-400 mesh) cation-exchange resin.
136 Solution samples (1–6 ml) were evaporated, then dissolved in 3 ml of 5 wt.% ultrapure HNO_3.
137 Just before separation, 1.5 ml of 100% electronics industry grade (EL-grade) methanol (Kanto
138 Chemical Co.) was added, yielding 4.5 ml of solution. After sample loading, 89 ml of 1 M
139 HNO_3:80% v/v methanol was passed through the resin; the first 5 ml was discarded and the
140 following 84 ml was collected as the Li fraction. Subsequently, 60 ml of 2 M
141 ultrapure100-grade (UP100-grade) HCl (Kanto Chemical Co.) was passed through the resin, the
142 first 45 ml was discarded, and the following 15 ml was collected as the Sr fraction. The Li and
143 Sr fractions were further separated in independent operations.

144 The second Li purification was carried out using a quartz glass column filled to a
145 height of 2 cm with 0.8 ml Bio-Rad AG50W X12 (200-400 mesh) cation-exchange resin. The
146 Li fraction was evaporated and dissolved in 0.2 ml of 0.25 M ultrapure HCl. Just before the

147 second column separation, 0.5 ml of 0.5 M HCl:80% v/v methanol was added. After sample
148 loading, 2 ml of 0.5 M HCl:80% v/v methanol was passed and discarded. Subsequently, 32 ml
149 of 1 M HCl:80% v/v methanol was passed and collected as the Li fraction. The Li contents of
150 recovered Li fraction have been measured from a comparison of the relative beam intensities of
151 the sample solution and L-SVEC standard solution, and we have confirmed that near 100% Li
152 was recovered during the two-step column separation. Both cation-exchange resins were reused
153 after repeated sequential cleaning with 6 M EL-grade HCl and Milli-Q H_2O. Before sample
154 separation, ultrapure HCl was passed through both resins. This is an important procedure to
155 determine $^{7}Li/^{6}Li$ ratios accurately (NISHIO and NAKAI, 2002). If high-purity acid is not used for
156 the last pass, the acquired $^{7}Li/^{6}Li$ ratios are subject to a matrix effect. This analytical procedure
157 results in a Li blank with less than 10 pg Li, far less than the amounts of Li in the analyzed
158 samples (25–6300 ng Li).

159 The second Sr purification was carried out using a polypropylene column that was
160 filled to a height of 2 cm with 1 ml Eichrom Sr resin (50–100 μm). The Sr fraction from the first
161 separation was evaporated and dissolved in 2 ml of 3 M UP100-grade HNO_3. After sample
162 loading, 6 ml of 3 M UP100-grade HNO_3, 6 ml of 7 M UP100-grade HNO_3, and 2 ml of 3 M

163 UP100-grade HNO_3 were passed sequentially and discarded. Then 10 ml of 0.05 M UP-grade
164 HNO_3 (50 ˚C) was passed and collected as the Sr fraction. This procedure results in a Sr blank
165 with less than 50 pg Sr, far less than the amounts of Sr in the analyzed samples (180–5400 ng
166 Sr).
167
168 *3.2.2. Mass Spectrometry*
169 The $^{7}Li/^{6}Li$ ratios were measured on the MC-ICP-MS equipped with a
170 high-sensitivity skimmer cone, "x-cones." The purified Li solution diluted in 2% ultrapure
171 HNO_3 to about 10 ng g^{-1} Li was introduced into the MC-ICP-MS through an Aridus desolvating
172 system (Cetac Technologies) with a microconcentric PTEE nebulizer (100 μl min^{-1}). Before
173 each sample and standard measurement, the beam intensities on *m/e* 6 and 7 of 2% HNO_3 were
174 measured as a background for 30 s. Subsequently, the beam intensity ratios on *m/e* 6 and 7 were
175 measured repeatedly 30 times (4 s per ratio) after 1 min of initial uptake of sample solution. A
176 sample injection time of less than 4 min requires 0.4 ml of sample solution, equivalent to 4 ng
177 Li. The Li standard solution (NIST L-SVEC) was measured before and after sample analyses to
178 correct for instrumental mass bias. The typical ^{7}Li intensity of the 10 ng g^{-1} Li standard solution

179 is 20 pA (a 2 V signal with the 10^{11} Ω resistor), which is much higher than background levels of
180 0.2 pA. The measured $^{7}Li/^{6}Li$ ratios are expressed as permil deviations from the NIST L-SVEC
181 standard: $\delta^{7}Li = [[^{7}Li/^{6}Li]_{sample}/[^{7}Li/^{6}Li]_{L\text{-}SVEC\ standard} - 1] \times 1000$. Uncertainty for the $\delta^{7}Li$ value
182 was better than ±0.4‰, as estimated from the long-term reproducibility, +8.28±0.39‰ (2 SD, *n*
183 = 47) during a period from May 2007 to May 2009 of our in-house Li standard (Kanto Chemical
184 Co.). Reproducibilities of replicate $\delta^{7}Li$ analyses for geological rock standards were also better
185 than ±0.4‰. The $\delta^{7}Li$ values of the rock standard JB2 have been reported in many papers, and
186 the average $\delta^{7}Li$ value was given by Rosner et al. (2007) as +4.78‰ (*n* = 12), which agrees with
187 our $\delta^{7}Li$ value of +4.60 ± 0.34‰ (2 SD, *n* = 4). Our $\delta^{7}Li$ value for the proposed seawater
188 standard IRMM BCR-403 was +31.3‰ (Table 2), which agrees with a previously reported
189 value of +31.0‰ (MILLOT et al., 2004) within the ±0.4‰ uncertainty.

190 The $^{87}Sr/^{86}Sr$ ratios were measured on the Triton TIMS after the purified 100–300
191 ng Sr samples were loaded on single tungsten filaments together with a tantalum activator
192 solution (BIRCK, 1986). Uncertainty for the $^{87}Sr/^{86}Sr$ ratio was better than ±0.000007, as
193 estimated from the long-term reproducibility, 0.7102507 ± 0.0000066 (2 SD, *n* = 36), during a
194 period from May 2007 to May 2009 of the NIST SRM 987 standard (80 ng Sr). Our $^{87}Sr/^{86}Sr$

195 ratio of rock standard JB2 was 0.7036785 ± 0.0000065 (2 SD, n = 4).

196

197 **4. RESULTS**

198 The δ^7Li and ^{87}Sr/^{86}Sr values of our water samples around Ontake volcano during the
199 observation period from 2000 to 2009 are listed in Table 2, together with chemical compositions.
200 The contents range from 0.57 μg/L to 2370 μg/L Li and from 17.8 μg/L to 4010 μg/L Sr (Table
201 2). The lowest contents of both Li and Sr were observed in sample AKG-03, which was
202 expected as it was river water rather than spring water. The Li content was 0.57 μg/L,
203 comparable to the flow-weighted mean world river water Li content of 1.5 μg/L (HUH et al.,
204 1998).

205 The isotopic values of our water samples ranged from −5.2‰ to +12.6‰ δ^7Li and
206 from 0.7056 to 0.7228 ^{87}Sr/^{86}Sr (Table 2). Previously reported δ^7Li values range from −0.1‰ to
207 +17.1‰ in hydrothermal-geothermal water (TOMASCAK et al., 2003; MILLOT and NEGREL,
208 2007), from +16.7‰ to +34.4‰ in lake water (TOMASCAK et al., 2003), and from +6.0‰ to
209 +37.5‰ in river water (HUH et al., 1998; TOMASCAK et al., 2003; VIGIER et al., 2009).
210 Accordingly, our δ^7Li values from KYK-03 (−2.4‰), KYK-09 (−3.4‰), KRB-09 (−4.9‰), and

KRB-07 (−5.2‰) were lower than previously reported geological fluid values.

Figure 2a shows the δ^7Li variation with distance between sampling site and the volcanic cone. The δ^7Li values of most samples ranged from +2‰ to +9‰. An exceptionally high value of +12.6‰ in sample AKG-03, the river water sample, is comparable to previously reported river water values from +6.0‰ to +37.5‰ (HUH et al., 1998; TOMASCAK et al., 2003; VIGIER et al., 2009). Relatively low δ^7Li values (the minimum is −5.2‰) were observed in several samples from the restricted area approximately 10 km from the volcano (Fig. 2a).

Figure 2b shows the $^{87}Sr/^{86}Sr$ variation with distance between sampling site and the volcanic cone. The $^{87}Sr/^{86}Sr$ ratios of samples within 20 km of the volcano tended to rise with distance from the volcanic cone (Fig. 2b). We found $^{87}Sr/^{86}Sr$ ratios lower than 0.707 only at sites YKW, NGG-C, and KRB less than 8 km from the volcanic cone (Table 2). The $^{87}Sr/^{86}Sr$ ratios of samples farther than 20 km ranged from 0.7083 to 0.7148 (Table 2).

We also analyzed Li and Sr isotopic compositions of fresh Ontake volcanic rocks that were drilled for core samples for paleomagnetic research (TANAKA and KOBAYASHI, 2003). The K-Ar ages of the samples ranged from 21 ka to 86 ka (MATSUMOTO and KOBAYASHI, 1995; MATSUMOTO and KOBAYASHI, 1999; TANAKA and KOBAYASHI, 2003). Table 3 shows

227 that the δ^7Li and $^{87}Sr/^{86}Sr$ values of these rocks ranged from +1.6‰ to +3.5‰ (+2.7 ± 1.5‰, 2

228 SD) and from 0.7055 to 0.7068 (0.7063 ± 0.0009, 2 SD), respectively.

229

230 **5. DISCUSSION**

231 **5.1. Spatial Distribution of Isotopic Ratios around Ontake Volcano**

232 *5.1.1. Volcanic Fluid in the Vicinity of the Volcanic Center*

233 The $^{87}Sr/^{86}Sr$ ratios of most water samples were higher than those in Ontake

234 volcanic rock, which range from 0.705 to 0.707 (Fig. 2b). Strontium ratios lower than 0.707

235 were observed only in sites YKW, NGG-C, and KRB, which are less than 8 km from the

236 volcanic cone (Fig. 2b). Of the water samples whose $^{87}Sr/^{86}Sr$ ratios are lower than 0.707, those

237 from sites YKW and NGG-C had δ^7Li values from +1.7‰ to +3.2‰ (Table 2), which are

238 comparable to those of the Ontake volcanic rock ranging from +1.6‰ to +3.5‰ (Table 3). In

239 sum, water samples with Li-Sr isotopic compositions similar to those of volcanic rock came

240 only from sites YKW and NGG-C, both of which are less than 5 km from the volcanic cone. It

241 is expected that the Li-Sr isotopic compositions of volcanic fluid that was interacted with

242 magma at high temperature are similar to those of volcanic rock. Researchers previously found

that in spring gases, $^{3}He/^{4}He$ ratios decrease with distance from the volcano, leading them to infer that volcanic helium with high $^{3}He/^{4}He$ passed through the rocks of the upper crust where they could have picked up helium with low $^{3}He/^{4}He$ (SANO et al., 1984; SANO et al., 1998; TAKAHATA et al., 2003). These helium isotopic results are consistent with the dominance of volcanic Li and Sr in the water samples from less than 5 km from the volcanic cone.

5.1.2. Low $\delta^{7}Li$ Fluid in Earthquake Swarm Region

Earthquake swarms have been beneath the three sites (KRB, KYK, and SRK) whose $\delta^{7}Li$ values were especially low (Fig. 3a). At the same time, electrical conductivity surveys have detected a low-resistivity fluid conduit beneath the KRB-KYK-SRK area (KASAYA et al., 2002; KASAYA and OSHIMAN, 2004) (Fig. 1). We therefore infer that the relatively low $\delta^{7}Li$ values observed in samples from sites KRB, KYK, and SRK reflect the influence of deep-seated fluids associated with crustal deformation beneath the southeast flank of Ontake volcano. Differences in $^{87}Sr/^{86}Sr$ ratios were not observed in samples from these three sites (Fig. 3b).

259 **5.2. Characteristics of Low δ^7Li Fluid**

260 *5.2.1. Evidence of Exposure to High Temperatures*

261 Both Si contents and Na/K ratios are useful indicators of the maximum temperature
262 that a fluid has experienced: Si contents increase and Na/K ratios decrease with the temperature
263 of rock–fluid interaction (FOURNIER and ROWE, 1966; FOURNIER and TRUESDELL, 1973;
264 GIGGENBACH, 1988). Figures 4a and 4b show the correlation between δ^7Li values and Si
265 content and between δ^7Li values and Na/K ratios, respectively. The samples from sites KRB,
266 KYK, and SRK had δ^7Li values that decreased with increasing Si contents and decreasing Na/K
267 ratios (data around dotted lines in Figs. 4) in a trend quite distinct from trends of the other
268 samples (data are underlain by grey shades in Figs. 4). These data suggest that low-δ^7Li fluids
269 recovered from sites KRB, KYK, and SRK have experienced high temperatures, although their
270 temperatures at the time of sampling were lower than 20 ˚C (Table 2).

271

272 *5.2.2. Non-surface Fluid*

273 The δ^7Li values of the samples from site SRK collected in 2000, 2005, and 2007
274 varied widely, from +1.1‰ to +4.9‰ (Table 2). Because these values were linearly correlated

with the Cl/Li ratios (Fig. 5a), we ascribe the temporal δ^7Li variation in these samples to a mixture of two components. Site SRK, being located near the river's edge, is more likely to be contaminated with near-surface meteoric water than the other sites. To examine this possibility, we analyzed a river water sample (SRK-2007-river) collected about 10 m upstream from the gas bubbling site where sample SRK-2007 was recovered: both samples were collected at the same time. The Cl/Li ratios of samples SRK-2007-river and SRK-2007 were 2100 and 240, respectively; thus, the Cl/Li ratio of the near-surface meteoric water was higher than that of the non-surface fluid. An exceptionally high Cl/Li ratio was also observed in sample AKG-03, which was extensively contaminated by river water (upper right corner of Fig. 5a).

Low δ^7Li values were also observed in samples from sites KRB and KYK. Those of the KRB samples were identical (−5.2‰ and −4.9‰) whereas those of the KYK samples varied widely (−2.4‰, −4.9‰, and +0.7‰). Because the δ^7Li values of the KYK samples were correlated linearly with the Cl/Li ratios (Fig. 5a), we ascribe the temporal δ^7Li variation in the KYK samples, like those from SRK, to binary mixing of near-surface meteoric water (high δ^7Li, high Cl/Li) and non-surface (deep) fluid (low δ^7Li, low Cl/Li).

The temporally varied $^{87}Sr/^{86}Sr$ ratios at each sampling site are also linearly

291 correlated with the Cl/Sr ratios (Fig. 5b). The Cl/Sr ratios of samples SRK-2007-river and
292 SRK-2007 were 210 and 29, respectively; thus, the Cl/Sr ratio of the near-surface meteoric
293 water is higher than that of the non-surface fluid.

294 As shown in Fig. 6a, a negative correlation between δ^7Li and ^{87}Sr/^{86}Sr was observed
295 in the SRK samples, including the river water sample. Consequently, we attribute the Li-Sr
296 isotopic trend of the SRK samples to binary mixing between near-surface meteoric water (high
297 δ^7Li, low ^{87}Sr/^{86}Sr) and non-surface fluid (low δ^7Li, high ^{87}Sr/^{86}Sr). We infer similar mixing in
298 the samples from site KYK (Fig. 6a).

299

300 **5.3. Li and Sr Isotopic Systematics of Non-surface Fluids**

301 *5.3.1. Identification Method for Non-surface Fluid*

302 Given that Li and Sr isotopic compositions of our water samples were affected by
303 contamination from near-surface meteoric water, we attempted to select samples free of this
304 contamination. The δ^7Li values of water samples with Cl/Li ratios less than 1100 were
305 approximately equal to those of non-surface fluids (Fig. 5a). The uncertainties in δ^7Li of these
306 water samples are expected to be ±0.5‰, as estimated from the δ^7Li difference of two SRK

307 samples with Cl/Li ratios of 240 and 1100 (Fig. 5a′). The $^{87}Sr/^{86}Sr$ ratios of water samples with
308 relatively low Cl/Sr ratios appeared not to be appreciably shifted by near-surface meteoric water
309 contamination (Fig. 5b). Then, we selected the $^{87}Sr/^{86}Sr$ ratios of water samples with Cl/Sr ratios
310 less than 350 to represent the non-surface fluid values (Fig. 5b). The uncertainties in $^{87}Sr/^{86}Sr$
311 ratios of these water samples are expected to be ±0.003, as estimated from the $^{87}Sr/^{86}Sr$
312 difference of two SRK samples whose Cl/Sr ratios are 30 and 210 (Fig. 5b). Because $^{87}Sr/^{86}Sr$
313 was constant regardless of varying Cl/Sr at sites KYK, DKS, NGG-C, and YY, the $^{87}Sr/^{86}Sr$
314 uncertainties of samples from these sites should be much smaller than ±0.003 (Fig. 5b).
315
316 *5.3.2. Inactive Earthquake Sites Samples*
317 On the basis of their Cl/Li and Cl/Sr ratios, we singled out water samples whose Li
318 and Sr isotopic ratios were minimally affected by meteoric water contamination to represent
319 non-surface fluids. As shown in Figure 3, earthquake swarms have been active beneath the three
320 sites (KRB, KYK, and SRK). Hereafter, this paper calls sampling sites other than the sites KRB,
321 KYK, and SRK as inactive earthquake sites. The Li and Sr isotopic data of non-surface fluids
322 from the inactive earthquake sites, as shown as grey shade in Fig. 6b, are distributed in a cluster.

As mentioned in section 5.1.1, the dominance of volcanic Li and Sr in the water samples from less than 5 km from the volcanic cone. Because only water samples from sites YKW and NGG-C, within 5 km of the volcanic cone, had Li and Sr isotopic compositions falling within the range of volcanic rock values (Fig. 6b), we estimated the δ^7Li and $^{87}Sr/^{86}Sr$ values of the Ontake volcanic fluid as +3‰ and 0.707, respectively, from the average values of the water samples from YKW and NGG-C.

As mentioned in section 4, the $^{87}Sr/^{86}Sr$ ratios of water samples within 20 km of the volcano tended to rise with distance from the volcanic cone (Fig. 2b). The non-surface fluid data (Cl/Li ratios less than 1100 and Cl/Sr ratios less than 350) also showed the $^{87}Sr/^{86}Sr$ increase with distance from the volcanic cone. The basement rocks of the Ontake region have distinctly higher $^{87}Sr/^{86}Sr$ ratios than Ontake volcanic rocks: the Mino sedimentary rock ranges from 0.715 to 0.730 (ASAHARA et al., 2006), the Naegi-Agematsu granite ranges from 0.729 to 0.750 (ASAHARA et al., 2006), and the Nohi rhyolite ranges from 0.710 to 0.736 (OKAMOTO et al., 1975). Then, we infer that the volcanic fluids with low $^{87}Sr/^{86}Sr$ ratios passed through basement rocks, where they could have picked up high $^{87}Sr/^{86}Sr$ strontium from the basement rocks of the Ontake region.

339 The δ^7Li values of non-surface fluids from the inactive earthquake sites, as shown as
340 grey shade in Fig. 6b, range from +2‰ to +7‰, while the $^{87}Sr/^{86}Sr$ ratios vary widely from
341 0.707 to 0.723. Thus, some non-surface fluids from the inactive earthquake sites have δ^7Li
342 values lower than the volcanic fluid (about +3‰, as discussed above in this section 5.3.2). As
343 well as Sr isotopic ratios, a plausible explanation therefore is that the lithium in water samples
344 with δ^7Li values higher than those of the volcanic rock derived from the basement rocks of the
345 Ontake region. The δ^7Li values of basement rocks of the Ontake region are unknown, while
346 those of the upper continental crust have been estimated from shales (−3‰ to +5‰), loess
347 (−3‰ to +5‰), granites (−3‰ to +3‰), and upper crustal composites (−5‰ to +3‰) from
348 North America, China, Europe, Australia, and New Zealand (TENG et al., 2004). The average
349 δ^7Li value of upper continental crust has been estimated as 0 ± 4‰ (2SD) (TENG et al., 2004),
350 which is rather lower than the average Ontake volcanic rock value, +3‰ (Table 3).
351 Lithium is found in an 8-coordinate position in most minerals and in a 4-coordinate
352 position in water. Because the lighter isotope has a greater affinity for the most highly
353 coordinated site, fluid–rock interactions lead to fluids with δ^7Li value higher than the associated
354 rock (OI et al., 1989; WENGER and ARMBRUSTER, 1991; ZACK et al., 2003; WUNDER et al.,

355 2006). The δ^7Li difference between fluid and rock ($\Delta^7Li_{fluid\text{-}rock}$) decreases with reaction
356 temperatures. The $\Delta^7Li_{fluid\text{-}rock}$ value is given as
357 $\Delta^7Li_{fluid\text{-}rock}$= 4.61×(1000/T [K])) – 2.48 (WUNDER et al., 2006; MARSCHALL et al., 2007).
358 (1)
359 As mentioned above, it is observed the dominance of volcanic Li and Sr in the water samples
360 from less than 5 km from the volcanic cone: Water samples from sites YKW and NGG-C,
361 within 5 km of the volcanic cone, had δ^7Li ranging from +1.7‰ to +3.2‰, equal to the Ontake
362 volcanic rock values (+1.6‰ to +3.4‰). The $\Delta^7Li_{fluid\text{-}rock}$ value is therefore +1.6‰ at maximum,
363 and the fluid-rock reaction temperature higher than 860˚C is estimated from the formula (1).
364 Thus, it is expected that the Ontake volcanic fluid reacted with the host volcanic rock (magma)
365 at high temperatures.
366 Subsequently, such high temperature volcanic fluid would become cold as it passes
367 through the basement rocks around magma reservoir. As mentioned above, the $^{87}Sr/^{86}Sr$ ratios of
368 the basement rocks are distinctly higher than those of volcanic fluid. We therefore estimated
369 that the Ontake upper crustal signature is δ^7Li of +6‰, from the sample DKS-07 whose
370 $^{87}Sr/^{86}Sr$ ratio was the highest among non-surface fluid data (Fig. 6b). Assuming the Ontake

371 upper crustal δ^7Li value of ±0‰, the $\Delta^7Li_{fluid\text{-}rock}$ value would be +6‰ and the fluid-rock
372 reaction temperature of 250˚C is estimated from the formula (1).

373 Interpretations mentioned above are not considered about effects from preferential
374 decomposition of rock-forming minerals. Each mineral in a source rock is going to have
375 different $^{87}Sr/^{86}Sr$ ratio due to in-situ ^{87}Sr-growth, therefore, it is expected that the $^{87}Sr/^{86}Sr$
376 discrepancy between fluid and whole rock occurs from preferential decomposition of minerals.
377 The experimental result indeed shows that the $^{87}Sr/^{86}Sr$ ratios of the fluids interacted with basalt
378 at high temperatures (>250˚C) range from 0.705 to 0.706, which are higher than the bulk-basalt
379 value, 0.703 (JAMES et al., 2003). However, more wide $^{87}Sr/^{86}Sr$ variation (0.707 to 0.723) has
380 been observed in the Ontake non-surface fluid that has once experienced high temperature.
381 Accordingly, we ascribe that the $^{87}Sr/^{86}Sr$ variation observed in the non-surface fluids from the
382 Ontake inactive earthquake sites is mainly a result of interaction between the volcanic fluid and
383 the basement rocks of the Ontake region.

384 In contrast to the $^{87}Sr/^{86}Sr$ ratio, it is expected that the $^7Li/^6Li$ ratios of every high
385 temperature rock-forming minerals are homogeneous, because both ^7Li and ^6Li are stable
386 isotopes and the Li isotope fractionation at per mil level does not occur during high-temperature

387 processes (TOMASCAK et al., 1999). Therefore, the Li isotopic difference between fluid and
388 whole rock is not caused by preferential decomposition of rock-forming minerals. As mentioned
389 above, the Li isotopic fractionation between fluid and rock is rather dependent on the
390 temperature.
391
392 *5.3.3. Active Earthquake Sites Samples*
393 As discussed in above section 5.3.2, the Li and Sr isotopic distribution of most
394 non-surface fluids can be explained as follows: volcanic fluids passed through the basement
395 rocks, where they could have acquired an upper crustal signature. This model, however, cannot
396 explain the Li and Sr isotopic distribution of non-surface fluids from active earthquake sites,
397 KRB, KYK, and SRK (Fig. 6b). Instead of volcanic fluid, another hot end-member fluid (fluid
398 X) is required to explain the Li and Sr isotopic data of non-surface fluids from the active
399 earthquake sites (Fig. 6b). Then, the Li and Sr isotopic distribution of non-surface fluids from
400 the active earthquake sites can be explained as follows: hot fluid X passed through the basement
401 rocks, where it could have acquired an upper crustal signature. We estimate the δ^7Li and
402 $^{87}Sr/^{86}Sr$ values of fluid X as below −5‰ and below 0.705, respectively, on the basis of the

403 non-surface fluid from site KRB.

404

405 **5.4. Origin of Fluid-X related to Earthquake Swarms**

406 The major basement rocks beneath the active earthquake region, the southeast flank
407 of Ontake volcano, are sedimentary rock and granite, whose $^{87}Sr/^{86}Sr$ ratios range from 0.715 to
408 0.750 (OKAMOTO et al., 1975; ASAHARA et al., 2006). The estimated $^{87}Sr/^{86}Sr$ ratio of fluid X is
409 much lower at 0.705, a value that cannot be produced by interaction with any of these basement
410 rocks. The $^{87}Sr/^{86}Sr$ ratio of fluid X is rather comparable to that of the Ontake volcanic rock,
411 whereas its δ^7Li value below −5‰ is distinctly lower than that of the Ontake volcanic rock. As
412 mentioned in section 5.3.2, fluid–rock interactions tend to raise the δ^7Li values of the fluid (OI
413 et al., 1989; WENGER and ARMBRUSTER, 1991; ZACK et al., 2003; WUNDER et al., 2007).
414 Because the δ^7Li values of Ontake volcanic rocks range from +1.6 to +3.5‰ (Table 3), fluid
415 δ^7Li values lower than +1.6‰ cannot be produced solely by interaction with the Ontake
416 volcanic rocks at any temperature. Then, the fluid X would be reacted with rock bodies with a
417 $^{87}Sr/^{86}Sr$ ratio of 0.705 and δ^7Li values below −5‰, but no such rock bodies have ever been
418 observed in island arc upper crust.

419 Many earthquake swarms have occurred beneath sites KRB, KYK, and SRK, where
420 low δ^7Li values were observed (Fig. 3a), and electrical conductivity data (Fig. 1c) suggest that
421 deep-seated fluid is rising from at least 10 km depth in this area (KASAYA et al., 2002; KASAYA
422 and OSHIMAN, 2004). The thickness of the crust in this region ranges from 30 km to 35 km, and
423 the lower boundary of the seismic upper crust is at a depth of approximately 16 km (ZHAO et al.,
424 1992; IIDAKA et al., 2003). We speculate that the fluid conduit beneath the KRB-KYK-SRK
425 area is connected to the lower crust, and we infer that fluid X is a lower crustal fluid.
426 Data from gabbroic inclusions suggest that the $^{87}Sr/^{86}Sr$ ratios of lower crustal rocks
427 beneath the northern Fossa Magna region (about 120 km north of Ontake volcano) range from
428 0.704 to 0.706 (SHUTO et al., 1988), which is consistent with the values for fluid X (0.705).
429 Although the δ^7Li value of the lower crust of an island arc is unknown, that of the lower
430 continental crust has been estimated using granulite-facies xenoliths from Australia and China
431 (TENG et al., 2008). Analyses of eight xenoliths that reached intermineral isotopic equilibria,
432 considered most likely to preserve the initial Li isotopic signature of the lower crust, suggest
433 that the lower continental crust is extremely heterogeneous, with δ^7Li ranging from −14‰ to
434 +14‰ (TENG et al., 2008). The distinctly low δ^7Li value of fluid X is within the range of these

435 data. Hamelin et al. (2009) also suggested that the δ^7Li value of a portion of lower continental
436 crust may be lower than −5‰, based on the observed δ^7Li variation (from 0‰ to +7‰) in a
437 suite of continental volcanic rocks from Chaine des Puys (French Massif Central).

438 The δ^7Li values of the non-surface fluids from sites KRB, KYK, and SRK also
439 decreased with the decrease in $^{87}Sr/^{86}Sr$ (Fig. 6b). This correlation can be explained by lower
440 crustal fluid (fluid X) passing through basement rocks where it acquired an upper crustal
441 signature. Although sites SRK and KYK are close (about 700 m apart), their non-surface Li and
442 Sr isotopic compositions were quite different (Fig. 6b). Samples at SRK were recovered from a
443 spring, while those at KYK were recovered from a well. It may be that the lower crustal fluid
444 signature is present in deep well water samples rather than in spring water samples.

445 As discussed in sections 5.2.2, we assumed both Cl/Li and Cl/Sr ratios of
446 non-surface fluids to be significantly lower than those of near-surface meteoric water. If the Li
447 and Sr isotopic compositions of the non-surface fluids from sites KRB, KYK, and SRK can be
448 explained by interaction of lower crustal fluid and upper crustal materials, then both Cl/Li and
449 Cl/Sr ratios of these fluids should be significantly lower than those of near-surface meteoric
450 water. Lower crustal fluids contain both Cl and Li in abundance (MARKL and BUCHER, 1998;

451 SVENSEN et al., 1999; SVENSEN et al., 2001), although their Sr contents are unknown. From
452 omphacite-hosted and garnet-hosted fluid inclusion data, it has been estimated that Cl/Li ratios
453 of lower crustal fluids range from 300 to 4000 (SVENSEN et al., 2001), distinctly lower than
454 those of water samples contaminated by near-surface water (the maximum is 110000).

455 Figure 7 shows a schematic illustration for non-surface fluid circulation beneath
456 studied region. As shown in this Fig. 7, we ascribe that the fluid-X associated with the
457 earthquake swarms is not simple volcanic fluid, but is rather influenced from the lower crust.
458 The origin of deep crustal fluid still remains unrevealed, but two possible origins are as follows:
459 The first possible origin is slab-derived aqueous fluid (Fig. 7), because of the shallow geometry
460 (70 km depth) of the subducting Philippine Sea plate beneath the studied area (KIMURA and
461 YOSHIDA, 1999; NAKAJIMA and HASEGAWA, 2007). The second possible origin is aqueous
462 fluid dehydrated (degassed) from the deep magma (Fig. 7). The aqueous fluids derived from
463 subducted slab and/or deep magma reacted with the lower crust, and then low δ^7Li and low
464 $^{87}Sr/^{86}Sr$ compositions of the fluid-X might be acquired (Fig. 7). However, further research is
465 necessary before we reveal origin of the fluid-X associated with the earthquake swarms.
466

6. CONCLUSIONS

The Li and Sr isotopic compositions of spring and well water samples around Ontake volcano are mainly accounted for by binary component mixing between near-surface meteoric water and non-surface fluid. Using data from water samples whose δ^7Li values and $^{87}Sr/^{86}Sr$ ratios were not greatly altered by near-surface meteoric water contamination, we estimated that the Li and Sr isotopic compositions of non-surface fluids are approximately equal to those in water samples whose Cl/Li ratios are less than 1100 and Cl/Sr ratios are less than 350.

The Li and Sr isotopic compositions of most non-surface fluids near Ontake can be explained as the result of volcanic fluids passing through basement rocks, where they acquired an upper crustal signature. The estimated δ^7Li and $^{87}Sr/^{86}Sr$ values of the Ontake volcanic fluid were +3‰ and 0.707, respectively, from the average values of the water samples from sites YKW and NGG-C within 5 km of the volcanic cone. The δ^7Li and $^{87}Sr/^{86}Sr$ values of the Ontake upper crustal end-member component, respectively +6‰ and 0.723, were estimated from sample DKS-07 whose $^{87}Sr/^{86}Sr$ ratio was the highest among non-surface fluid samples.

We observed anomalous Li and Sr isotopic compositions in non-surface fluids from

483 sites KRB, KYK, and SRK above vigorous earthquake swarms. We propose another
484 end-member fluid (fluid X) for these sites. Fluid X must have been produced by interaction with
485 rocks with $^{87}Sr/^{86}Sr$ ratios of 0.705 and $\delta^{7}Li$ values below −5‰, a combination not found in
486 upper crustal samples from the island arc. Given that a low-resistivity fluid conduit leads from
487 the deep crust to the surface beneath the earthquake swarm region (KASAYA et al., 2002;
488 KASAYA and OSHIMAN, 2004), we consider fluid X to be a lower crustal fluid. Our new Li and
489 Sr isotopic data suggest that the fluid associated with the earthquake swarms beneath the
490 southeast flank of Ontake volcano is not a simple volcanic fluid, but rather is influenced by the
491 lower crust.
492
493 *Acknowledgements*. We thank R. Hirose, K. Nagaishi, J. Matsuoka, and T. Noguchi for
494 analytical support, Y. Yamamoto and H. Tanaka for providing the volcanic rock samples, and T.
495 Kim for advice about Li isotope analyses. Thoughtful and constructive reviews by R. Halama, P.
496 Tomascak, J. Yamamoto, and anonymous referees helped to clarify the presentation, and an
497 editorial handling by T.M. Harrison is gratefully acknowledged. K. Kiyota, K. Shirai, and D. L.
498 Pinti assisted in sampling, H. Nakamichi provided map data, and K. Kasaya provided helpful

499 unpublished information on the study area. This study was supported by a Grant-in-Aid for
500 Scientific Research to Y. Nishio (Nos. 16740309 and 22109511) from the Ministry of Education,
501 Culture, Sports, Science and Technology of Japan. Nishio thanks the late George Igarashi for
502 influencing him to advance into crustal fluid science.

503

504 References

505 Asahara, Y., Ishiguro, H., Tanaka, T., Yamamoto, K., Mimura, K., Minami, M. and Yoshida, H.
506 (2006) Application of Sr isotopes to geochemical mapping and provenance analysis:
507 The case of Aichi Prefecture, central Japan. *Applied Geochemistry* **21**, 419-436.
508 Birck, J. L. (1986) Precision K-Rb-Sr isotopic analysis: Application to Rb-Sr chronology. *Chem.*
509 *Geol.* **56**, 73-83.
510 Fournier, R. O. and Rowe, J. J. (1966) Estimation of underground temperatures from the silica
511 content of water from hot springs and wet-steam wells. *Am J Sci* **264**, 685-697.
512 Fournier, R. O. and Truesdell, A. H. (1973) An empirical Na-K-Ca geothermometer for natural
513 waters. *Geochim. Cosmochim. Acta* **37**, 1255-1275.
514 Geological Survey of Japan, A. G., 1995. Geological Map of Japan 1:2,000,000 (Images)
515 Version. 2.0.
516 Giggenbach, W. F. (1988) Geothermal Solute Equilibria - Derivation of Na-K-Mg-Ca
517 Geoindicators. *Geochim. Cosmochim. Acta* **52**, 2749-2765.
518 Hamelin, C., Seitz, H.-M., Barrat, J.-A., Dosso, L., Maury, R. C. and Chaussidon, M. (2009) A
519 low δ^{7}Li lower crustal component: Evidence from an alkalic intraplate volcanic series
520 (Chaine des Puys, French Massif Central). *Chem. Geol.* **266**, 214-226.
521 Huh, Y., Chan, L.-H., Zhang, L. and Edmond, J. M. (1998) Lithium and its isotopes in major
522 world rivers: implications for weathering and the oceanic budget. *Geochim. Cosmochim.*
523 *Acta* **62**, 2039-2051.
524 Iidaka, T., Iwasaki, T., Takeda, T., Moriya, T., Kumakawa, I., Kurashimo, E., Kawamura, T.,
525 Yamazaki, F., Koike, K. and Aoki, G. (2003) Configuration of subducting Philippine

526 Sea plate and crustal structure in the central Japan region. *Geophys. Res. Lett.* **30**, -.
527 Iio, Y., Sagiya, T., Kobayashi, Y. and Shiozaki, I. (2002) Water-weakened lower crust and its
528 role in the concentrated deformation in the Japanese Islands. *Earth Planet. Sci. Lett.* **203**,
529 245-253.
530 James, R. H., Allen, D. E. and Jr., W. E. S. (2003) An experimental study of alteration of
531 oceanic crust and terrigenous sediments at moderate temperatures (51 to 350˚C):
532 insights as to chemical processes in near-shore ridge-flank hydrothermal systems.
533 *Geochim. Cosmochim. Acta* **67**, 681-691.
534 Jeffcoate, A. B., Elliott, T., Thomas, A. and Bouman, C. (2004) Precise, small sample size
535 determinations of lithium isotopic compositions of geological reference materials and
536 modern seawater by MC-ICP-MS. *Geostandards Geoanal. Res.* **28**, 161-172.
537 Kasaya, T. and Oshiman, N. (2004) Lateral inhomogeneity deduced from 3-D magnetotelluric
538 modeling around the hypocentral area of the 1984 Western Nagano Prefecture
539 earthquake, central Japan. *Earth Planets and Space* **56**, 547-552.
540 Kasaya, T., Oshiman, N., Sumitomo, N., Uyeshima, M., Iio, Y. and Uehara, D. (2002)
541 Resistivity structure around the hypocentral area of the 1984 Western Nagano
542 Prefecture earthquake in central Japan. *Earth Planets and Space* **54**, 107-118.
543 Kimata, F., Miyajima, R., Murase, M., Darwaman, D., Ito, T., Ohata, Y., Irwan, M., Takano, K.,
544 Ibrahim, F., Koyama, E., Tsuji, H., Takayama, T., Uchida, K., Okada, J., Solim, D. and
545 Anderson, H. (2004) Ground uplift detected by precise leveling in the Ontake
546 earthquake swarm area, central Japan in 2002-2004. *Earth Planets and Space* **56**,
547 E45-E48.
548 Kimura, J. and Yoshida, T. (1999) Magma plumbing system beneath Ontake Volcano, central
549 Japan. *Island Arc* **8**, 1-29.
550 Markl, G. and Bucher, K. (1998) Composition of fluids in the lower crust inferred from
551 metamorphic salt in lower crustal rocks. *Nature* **391**, 781-783.
552 Marschall, H. R., Pogge von Strandmann, P. A. E., Seitz, H.-M., Elliott, T. and Niu, Y. (2007)
553 The lithium isotopic composition of orogenic eclogites and deep subducted slabs. *Earth*
554 *Planet. Sci. Lett.* **262**, 563-580.
555 Matsumoto, A. and Kobayashi, T. (1995) K-Ar Age-Determination of Late Quaternary
556 Volcanic-Rocks Using the Mass Fractionation Correction Procedure - Application to the
557 Younger Ontake Volcano, Central Japan. *Chem. Geol.* **125**, 123-135.
558 Matsumoto, A. and Kobayashi, T. (1999) K-Ar ages of the older Ontake volcanic products,

559 Ontake volcano, central Japan: Reappraisal of the volcanic history based on the
560 radiometric data. *Bull. Volcanol. Soc. Japan* **44**, 1-12.
561 Millot, R., Guerrot, C. and Vigier, N. (2004) Accurate and high-precision measurement of
562 lithium isotopes in two reference materials by MC-ICP-MS. *Geostandards Geoanal.*
563 *Res.* **28**, 153-159.
564 Millot, R. and Negrel, P. (2007) Multi-isotopic tracing (δ^{7}Li, δ^{11}B, ^{87}Sr/^{86}Sr) and chemical
565 geothermometry: evidence from hydro-geothermal systems in France. *Chem. Geol.* **244**,
566 664-678.
567 Millot, R., Negrel, P. and Petelet-Giraud, E. (2007) Multi-isotopic (Li, B, Sr, Nd) approach for
568 geothermal reservoir characterization in the Limagne Basin (Massif Central, France).
569 *Applied Geochemistry* **22**, 2307-2325.
570 Nakajima, J. and Hasegawa, A. (2007) Subduction of the Philippine Sea plate beneath
571 southwestern Japan: Slab geometry and its relationship to arc magmatism. *Journal of*
572 *Geophysical Research-Solid Earth* **112**, -.
573 Nakamichi, H., Kumagai, H., Nakano, M., Okubo, M., Kimata, F., Ito, Y. and Obara, K. (2009)
574 Source mechanism of a very-long-period event at Mt Ontake, central Japan: Response
575 of a hydrothermal system to magma intrusion beneath the summit. *J. Volcanol.*
576 *Geotherm. Res.* **187**, 167-177.
577 Nishio, Y. and Nakai, S. (2002) Accurate and precise lithium isotopic determinations of igneous
578 rock samples using multi-collector inductively coupled plasma mass spectrometry. *Anal.*
579 *Chim. Acta* **456**, 271-281.
580 Nishio, Y., Nakai, S., Yamamoto, J., Sumino, H., Matsumoto, T., Prikhod'ko, V. S. and Arai, S.
581 (2004) Lithium isotopic systematics of the mantle-derived ultramafic xenoliths:
582 implications for EM1 origin. *Earth Planet. Sci. Lett.* **217**, 245-261.
583 Oi, T., Nomura, M., Musashi, M., Ossaka, T., Okamoto, M. and Kakihana, H. (1989) Boron
584 isotopic compositions of some boron minerals. *Geochim. Cosmochim. Acta* **53**,
585 3189-3195.
586 Okamoto, K., Nohda, S., Masuda, Y. and Matsumoto, T. (1975) Significance of Cs/Rb ratios in
587 volcanic rocks as exemplified by the Nohi Rhyolite complex, Central Japan. *Geochem.*
588 *J.* **9**, 201-210.
589 Rosner, M., Ball, L., Peucker-Ehrenbrink, B., Blusztajn, J., Bach, W. and Erzinger, J. (2007) A
590 simplified, accurate and fast method for lithium isotope analysis of rocks and fluids, and
591 δ^{7}Li values of seawater and rock reference materials. *Geostandards Geoanal. Res.* **31**,

77-88.

Sano, Y., Nakamura, Y., Wakita, H., Urave, A. and Tominaga, T. (1984) Helium-3 emission related to volcanic activity. *Science* **224**, 150-151.

Sano, Y., Nishio, Y., Sasaki, S., Gamo, T. and Nagao, K. (1998) Helium and carbon isotope systematics at Ontake volcano, Japan. *J. Geophys. Res.* **103**, 23863-23873.

Seyfried, W. E., Janecky, D. R. and Mottl, M. J. (1984) Alteration of the Oceanic-Crust - Implications for Geochemical Cycles of Lithium and Boron. *Geochim. Cosmochim. Acta* **48**, 557-569.

Shuto, K., Kagami, H., Shimazu, M. and Yano, T. (1988) Sr and Nd isotopic study of gabbroic inclusions in calc-alkaline andesites from the northern Fossa Magna region, Central Japan. *Journal of Mineralogy, Petrology, and Economic Geology* **83**, 77-84.

Shuto, T. and Otsuka, T. (2004) Late Jurassic-earliest Cretaceous accretionary complex of the eastern Mino Terrane, central Japan: Radiolarian age and imbricate structure of the Misogawa Complex. *J. Geol. Soc. Japan* **110**, 67-84.

Svensen, H., Jamtveit, B., Banks, D. A. and Austrheim, H. (2001) Halogen contents of eclogite facies fluid inclusions and minerals: Caledonides, western Norway. *Journal of Metamorphic Geology* **19**, 165-178.

Svensen, H., Jamtveit, B., Yardley, B., Engvik, A. K., Austrheim, H. and Broman, C. (1999) Lead and bromine enrichment in eclogite-facies fluids: Extreme fractionation during lower-crustal hydration. *Geology* **27**, 467-470.

Takahata, N., Yokochi, R., Nishio, Y. and Sano, Y. (2003) Volatile element isotope systematics at Ontake volcano, Japan. *Geochem. J.* **37**, 299-310.

Tanaka, A. and Ito, H. (2002) Temperature at base of the seismogenic zone and its relationship to the focal depth of Western Nagano Prefecture area (in Japanese). *J. Seism. Soc. Japan (Zishin)* **55**, 1-10.

Tanaka, H. and Kobayashi, T. (2003) Paleomagnetism of the late Quaternary Ontake Volcano, Japan: directions, intensities, and excursions. *Earth Planets and Space* **55**, 189-202.

Teng, F.-Z., Rudnick, R. L., McDonough, W. F., Gao, S., Tomascak, P. B. and Liu, Y. (2008) Lithium isotopic composition and concentration of the deep continental crust. *Chem. Geol.* **255**, 47-59.

Teng, F. Z., McDonough, W. F., Rudnick, R. L., Dalpe, C., Tomascak, P. B., Chappell, B. W. and Gao, S. (2004) Lithium isotopic composition and concentration of the upper continental crust. *Geochim. Cosmochim. Acta* **68**, 4167-4178.

625 Tomascak, P. B., Carlson, R. W. and Shirey, S. B. (1999) Accurate and precise determination of
626 Li isotopic compositions by multi-collector sector ICP-MS. *Chem. Geol.* **158**, 145-154.
627 Tomascak, P. B., Hemming, N. G. and Hemming, S. R. (2003) The lithium isotopic
628 composition of waters of the Mono Basin, California. *Geochim. Cosmochim. Acta* **67**,
629 601-611.
630 Vigier, N., Gislason, S. R., Burton, K. W., Millot, R. and Mokadem, F. (2009) The relationship
631 between riverine lithium isotope composition and silicate weathering rates in Iceland.
632 *Earth Planet. Sci. Lett.* **287**, 434-441.
633 Wenger, M. and Armbruster, T. (1991) Crystal chemistry of lithium: oxygen coordination and
634 bonding. *European Journal of Mineralogy* **3**, 387-399.
635 Wunder, B., Meixner, A., Romer, R. L., Feenstra, A., Schettler, G. and Heinrich, W. (2007)
636 Lithium isotope fractionation between Li-bearing staurolite, Li-mica and aqueous
637 fluids: An experimental study. *Chem. Geol.* **238**, 277-290.
638 Wunder, B., Meixner, A., Romer, R. L. and Heinrich, W. (2006) Temperature-dependent
639 isotopic fractionation of lithium between clinopyroxene and high-pressure hydrous
640 fluids. *Contrib. Mineral. Petrol.* **151**, 112-120.
641 You, C.-F., Castillo, P. R., Gieskes, J. M., Chan, L. H. and Spivack, A. J. (1996) Trace element
642 behavior in hydrothermal experiments: Implications for fluid processes at shallow
643 depths in subduction zones. *Earth Planet. Sci. Lett.* **140**, 41-52.
644 Zack, T., Tomascak, P. B., Rudnick, R. L., Dalpe, C. and McDonough, W. F. (2003) Extremely
645 light Li in orogenic eclogites: The role of isotope fractionation during dehydration in
646 subducted oceanic crust. *Earth Planet. Sci. Lett.* **208**, 279-290.
647 Zhao, D., Horiuchi, S. and Hasegawa, A. (1992) Seismic Velocity Structure of the Crust
648 beneath the Japan Islands. *Tectonophysics* **212**, 289-301.
649

650

650 Figure Captions

651 Fig. 1

652 Locations of sampling sites (open circles) and geology in the Ontake volcano area (a). The
653 epicenter of the 1984 western Nagano Prefecture earthquake (M6.8) and the causative fault are
654 shown as a star and dashed line, respectively. Dots are epicenters of earthquakes during
655 2001–2005 at depths of –1 to 40 km (NAKAMICHI et al., 2009). The electrical conductivity
656 profiles along X–X′ (b) and Y–Y′ (c) are from Kasaya et al. (2002). Circles in (b) and (c) are
657 earthquake hypocenters during the period October–December 1995. A low-resistivity fluid
658 conduit from deep crust to the surface is inferred beneath the southeast flank of Ontake volcano
659 near this earthquake swarm region (KASAYA et al., 2002; KASAYA and OSHIMAN, 2004).

660

661 Fig. 2

662 Variations of δ^7Li values (a) and $^{87}Sr/^{86}Sr$ ratios (b) with distance from the volcanic cone. The
663 large open circles show the non-surface fluid data, defined by Cl/Li ratios less than 1100 and
664 Cl/Sr ratios less than 350. The dotted line loops are around the active earthquake site data and
665 the weak grey shades underlay inactive earthquake site data.

666

667 Fig. 3

668 Correlations between δ^7Li values and the number of earthquakes (a) and between $^{87}Sr/^{86}Sr$ ratios

669 and the number of earthquakes (b). Earthquakes selected from the Japan Meteorological Agency

670 earthquake catalog were bigger than M1, shallower than 30 km, within 1 km of each sampling

671 site, and occurred from January 1, 1995 to November 1, 2009. Earthquake swarms have

672 occurred beneath sites KRB, KYK, and SRK, where relatively low δ^7Li values were observed.

673

674 Fig. 4

675 Correlations between δ^7Li value and Si content (a) and between δ^7Li value and Na/K weight

676 ratio (b). The Si contents and Na/K weight ratios respectively increase and decrease with the

677 temperature of rock–fluid interaction (FOURNIER and ROWE, 1966; FOURNIER and TRUESDELL,

678 1973; GIGGENBACH, 1988). The dotted line loops and the weak grey shades are as same as those

679 in Fig. 2. The δ^7Li values of the active earthquake site samples decreased with increasing Si

680 contents and decreasing Na/K ratios (data around dotted lines), trends that differ strongly from

681 those of the inactive earthquake site samples (data are underlain by grey shades).

682

683 Fig. 5

684 Correlations between Cl/Li weight ratio and δ^7Li value (a) and between Cl/Sr weight ratio and

685 $^{87}Sr/^{86}Sr$ ratio (b). Fig. 5a′ is an enlargement of Fig. 5a. Different linear Cl/Li-δ^7Li correlations

686 were observed in samples KYK and SRK (a). Different linear Cl/Sr-$^{87}Sr/^{86}Sr$ correlations were

687 also observed in samples KYK, SRK, DKS, KKH-A, NGG-C, and YY (b). We infer that these

688 reflect binary component mixing between near-surface meteoric water (high Cl/Li, high Cl/Sr)

689 and non-surface fluid (low Cl/Li, low Cl/Sr).

690

691 Fig. 6

692 Correlations between $^{87}Sr/^{86}Sr$ ratio and δ^7Li value for all analyzed fluid samples (a) and for

693 non-surface fluids (b). Non-surface fluid data were selected from water samples with Cl/Li

694 ratios less than 1100 and Cl/Sr ratios less than 350, showing relatively little contamination by

695 near-surface meteoric water. Fig. 6b also shows $^{87}Sr/^{86}Sr$ ratios and δ^7Li values of the Ontake

696 volcanic rocks analyzed in this study (Table 3). The dotted line loops and the weak grey shades

697 are as same as those in Fig. 2.

698

699 Fig. 7

700 A schematic illustration for non-surface fluid circulation beneath studied region. We ascribe that

701 the fluid-X associated with the earthquake swarms is not simple volcanic fluid, but is rather

702 influenced from the lower crust. We have speculated that this fluid-X associated with the

703 earthquake swarms may be originated from aqueous fluids derived from subducted slab and/or

704 deep magma.

705

Table 1
Location of sampling sites of spring and well water samples analyzed in this study

Sampling site	Latitude (˚N)	Longitude (˚E)	Distance from cone (km)	Type*	Sampling year	
					fluid	gas$
AKG	35.99	137.40	12.1	N	2003	1981-2007
DKS	35.82	137.63	16.5	N	1993-2007	1993-2007
KKH	35.81	137.69	21.9			
KKH-A				N	2000-2009	1981-2009
KKH-B				P	2005	2005
KNS	35.91	137.56	7.4			
KNS-A				N	2000-2003	1981-2003
KNS-B				N	2005-2009	2005-2009
KNS-C				P	2009	-
KYK	35.88	137.60	10.7	P	2003-2009	2003-2009
KRB	35.86	137.55	7.4	P	2007-2009	2007-2009
NGG	35.93	137.45	4.5			
NGG-A				N	-	1981-1993
NGG-B				P	2000	1996-2000
NGG-C				N	2003-2009	2003-2009
OTK	35.84	137.53	7.1	N	2009	2009
SRK	35.87	137.60	11.0	N	2000-2007	1985-2007
SJM	35.78	137.69	23.5	N	2000-2007	1981-2009
YKW	35.89	137.51	2.7	N	2007	1993-2007
YY	35.91	137.31	11.5	N	2000-2009	1981-2009

*: N= natural flow water; P= water pumped up.
$: The gas data before 2000 have been already reported in Sano et al. (1984;1986;1998) and Takahata et al. (2003).

Table 2
Li and Sr isotopic compositions and chemical compositions of spring and well water samples from Ontake area

Sample name	Sampling date	Temperature (˚C)	pH	$\delta^7Li^{\$}$ (‰)	$^{87}Sr/^{86}Sr^{\$}$	$Li^{\#}$ (μg/L)	$Rb^{\#}$ (μg/L)	$Sr^{\#}$ (μg/L)	$Si^{\#}$ (mg/L)	$K^{\#}$ (mg/L)	$Ca^{\#}$ (mg/L)	$Mg^{\#}$ (mg/L)	$Na^{\#}$ (mg/L)	$Cl^{\#}$ (mg/L)
AKG-03	June 2003	11.9	7.74	12.6	0.709228	0.57	0.88	17.8	5.32	0.78	25.1	1.06	3.80	63.0
DKS-00	June 2000	15.8	5.57	5.45	0.722624	63.2	1.89	133	20.7	0.30	71.1	14.8	20.0	79.6
DKS-03	June 2003	13.7	5.87	5.44	0.722757	136	3.97	351	35.6	1.17	205	42.1	54.4	151
DKS-05	June 2005	-	3.30	4.99	0.722773	72.2	2.45	129	23.8	0.63	71.3	14.5	22.1	87.8
DKS-07	June 2007	12.3	5.83	5.72	0.722762	108	3.28	258	30.2	1.03	129	26.4	35.2	3.71
KKH-A-00	June 2000	16.0	4.92	3.90	0.708333	4.26	6.64	126	27.9	1.57	12.2	2.64	6.29	94.6
KKH-A-03	June 2003	17.8	4.91	6.45	0.708325	6.64	7.86	186	31.5	2.91	17.2	3.42	8.98	185
KKH-A-07	June 2007	14.9	5.01	6.67	0.708633	6.65	7.57	173	35.2	3.52	16.6	3.57	11.6	9.25
KKH-A-09	July 2009	15.2	5.12	5.92	0.708500	5.66	7.99	169	33.0	3.42	14.8	2.86	10.8	6.96
KKH-B-05	June 2005	-	4.67	1.87	0.713345	110	20.3	122	34.5	4.08	38.6	6.63	21.7	79.9
KNS-A-00	June 2000	27.7	6.04	4.79	0.710276	1000	189	807	54.2	57.9	132	82.7	422	276
KNS-A-03	June 2003	27.6	6.10	4.12	0.710271	1030	199	848	62.3	65.4	149	93.3	474	281
KNS-B-05	June 2005	24.7	6.07	6.29	0.707925	631	113	478	60.1	39.1	84.5	53.1	279	198
KNS-B-07	June 2007	23.7	6.19	6.33	0.707709	537	99.0	405	53.7	32.1	67.0	42.5	224	103
KNS-B-09	July 2009	22.4	6.30	6.16	0.708014	467	85.5	342	47.9	26.8	58.2	36.4	211	83.1
KNS-C-09	July 2009	37.1	6.76	3.23	0.716137	2370	331	4010	32.1	71.5	353	214	738	682
KRB-07	June 2007	11.0	5.77	-5.17	0.705603	23.9	36.5	646	47.8	12.7	71.5	28.7	12.8	1.51
KRB-09	July 2009	12.6	5.69	-4.91	0.705577	21.6	33.7	616	41.2	9.6	61.2	23.5	10.6	0.73
KYK-03	June 2003	14.8	5.83	-2.35	0.712781	5.77	4.65	31.6	36.2	1.53	4.86	2.37	3.29	44.4
KYK-05	June 2005	13.8	5.08	0.70	0.712051	5.07	5.82	33.2	35.2	2.05	5.56	2.67	5.40	125
KYK-09	July 2009	13.6	7.01	-3.37	0.711864	5.71	7.57	46.6	37.4	2.95	6.71	3.89	6.29	0.60
NGG-B-00	June 2000	49.4	6.23	3.76	0.709084	1090	117	924	88.1	60.5	149	90.1	377	188
NGG-C-03	June 2003	34.0	6.00	2.82	0.706817	310	63.5	473	74.0	28.9	85.7	48.2	165	284
NGG-C-05	June 2005	36.8	5.89	3.05	0.706842	316	64.4	464	74.0	30.9	87.6	49.5	174	110
NGG-C-07	June 2007	36.2	6.15	3.16	0.706840	321	66.2	504	76.7	30.1	88.6	49.9	169	69.7
NGG-C-09	July 2009	37.1	6.22	2.99	0.706845	320	66.0	481	74.0	28.2	85.0	47.4	178	78.5
OTK-09	July 2009	20.7	6.30	6.96	0.714595	817	56.4	1360	51.9	31.7	194	78.3	405	216
SJM-00	June 2000	16.7	5.53	9.02	0.714771	8.51	4.95	54.2	6.66	0.74	10.1	1.81	4.92	21.5
SJM-03	June 2003	13.4	5.93	8.36	0.710533	132	13.1	230	21.7	3.59	55.6	7.44	49.9	190
SJM-05	June 2005	21.6	5.15	4.30	0.710850	47.3	7.63	101	14.6	2.48	20.4	2.58	13.5	137
SJM-07	June 2007	17.0	5.46	5.66	0.710597	96.1	8.63	140	19.1	2.88	31.8	4.22	24.9	19.3
SRK-00	June 2000	14.2	6.80	4.89	0.709571	5.02	3.59	31.0	9.31	0.34	3.63	1.17	1.99	96.5
SRK-05	June 2005	16.5	5.00	1.55	0.716163	32.6	8.32	164	17.9	2.33	18.5	3.93	11.6	34.9
SRK-07	June 2007	15.7	5.36	1.08	0.717768	50.1	12.2	415	20.1	4.13	41.0	8.48	21.4	12.0
SRK-07-river	June 2007	13.8	5.23	2.83	0.715157	15.7	6.70	162	20.4	2.63	21.9	4.15	8.3	33.5
YKW-07	June 2007	30.1	5.31	1.73	0.706434	102	93.1	366	64.9	23.2	95.3	23.0	133	87.5
YY-00	June 2000	13.2	5.95	2.55	0.710479	76.6	13.6	39.5	4.85	0.68	6.08	0.53	20.8	64.3
YY-03	June 2003	13.8	5.58	3.82	0.710782	507	59.2	190	10.0	5.38	18.3	1.53	132	193
YY-05	June 2005	15.9	5.65	3.19	0.710794	652	72.3	213	11.4	7.01	20.6	1.79	170	119
YY-07	June 2007	13.5	5.77	4.11	0.710832	1150	115	361	13.9	11.4	29.3	2.49	279	166
YY-09	July 2009	14.1	5.99	4.56	0.710351	106	12.8	70.5	5.11	1.80	9.90	0.52	33.8	18.6
Fluid Standard						(μg/L)	(μg/L)	(mg/L)	(mg/L)	(mg/L)	(mg/L)	(g/L)	(g/L)	(g/L)
BCR-403				31.3	0.709180	179	111	7.58	4.44	391	393	1.28	10.5	19.8

$: Li and Sr isotopic compositions were detrmined by MC-ICP-MS and TIMS, respectively.
#: Li, Rb, and Sr contents were by ICP-MS; Si contents were by ICP-AES; K, Ca, Mg, Na, and Cl contents were by IC.

Table 3
Li and Sr isotopic compositions of Ontake volcanic rocks[$] (bulk)

Sample name	K-Ar age (ka)	δ^7Li[#] (‰)	$^{87}Sr/^{86}Sr$[*]
OT13	59±7[a]	3.37	0.705476
OT37	66±5[a]	1.82	0.706266
OT40	48±4[a]	3.26	0.706508
OT43	36±3[a]	2.70	0.706215
OT49	81±23[b]	3.46	0.706708
OT53	21±5[c]	2.72	0.706008
OT63	86±6[d]	1.61	0.706812
Mean		2.70	0.706285
2SD		1.49	0.000910

$: fresh drilled core samples for paleomagnetic research
#: analyzed by MC-ICP-MS
*: analyzed by TIMS
a: reported in Tanaka and Kobayashi (2002)
b: reported in Matsumoto and Kobayashi (1999); TKN-29, TKN-46
c: reported in Matsumoto and Kobayashi (1995); SNTK-72
d: reported in Matsumoto and Kobayashi (1995); NGRG-240

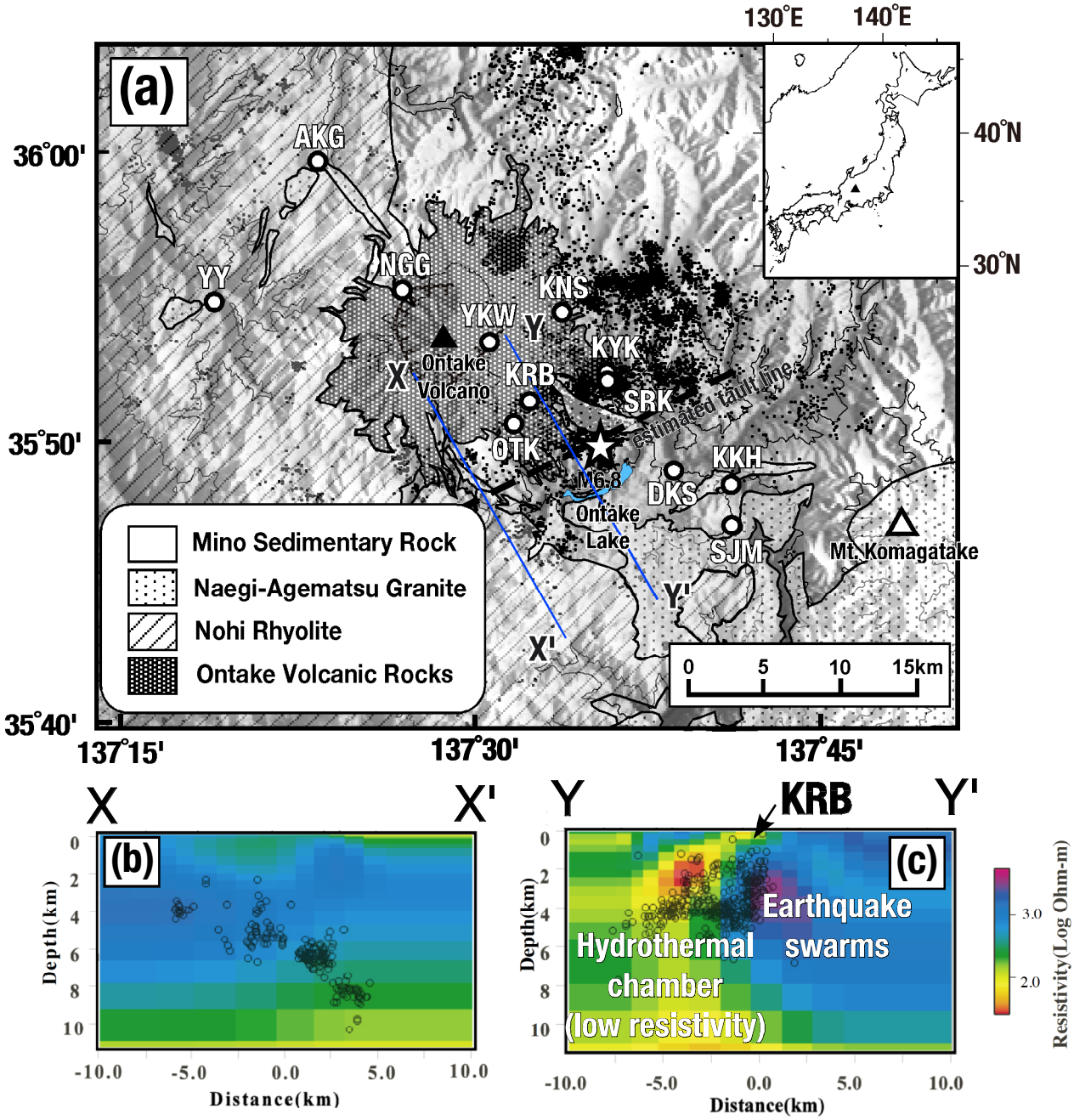

2D electric conductivity results by Kasaya et al. (2002)

Figure 1/ Nishio et al.

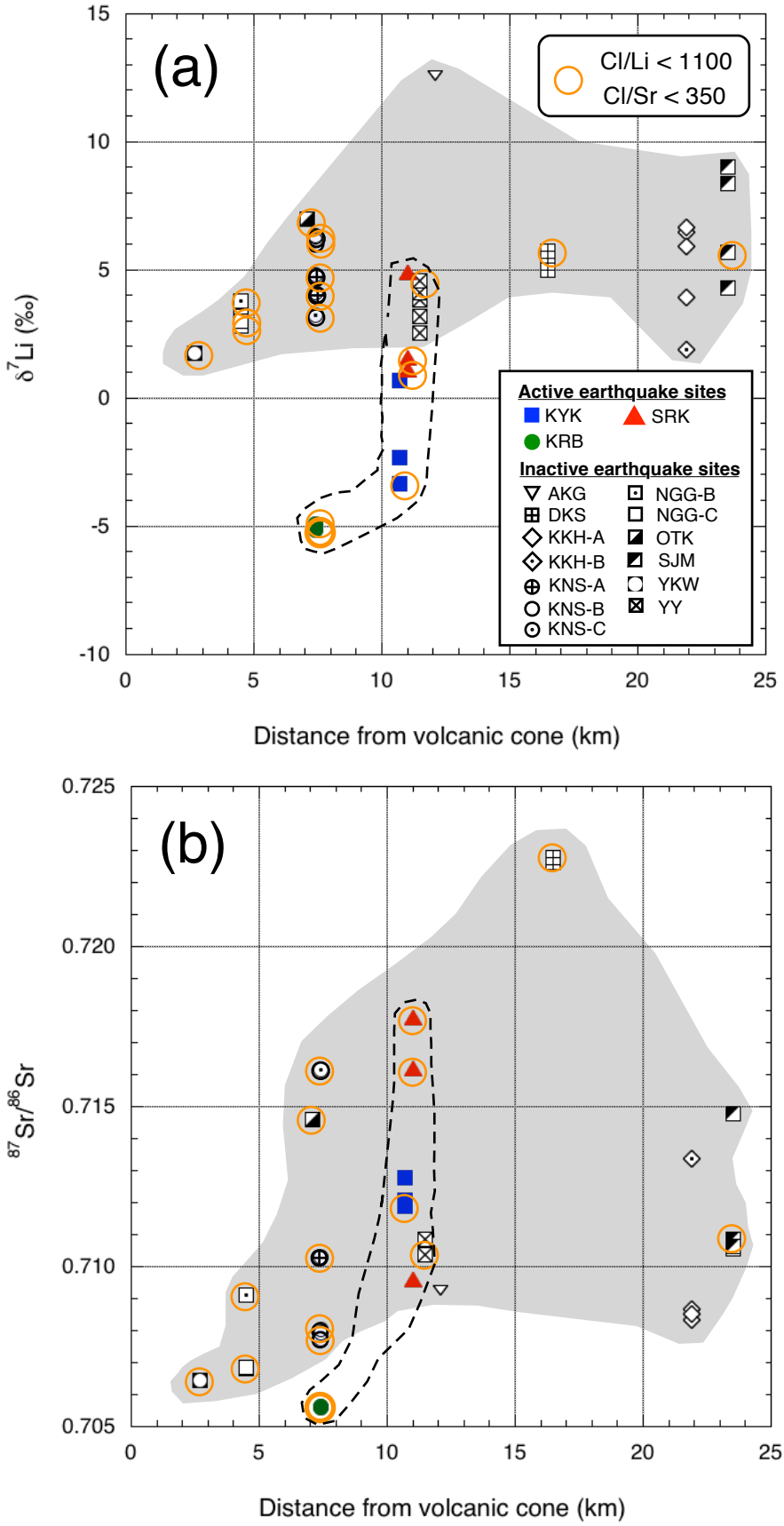

Figure 2 / Nishio et al.

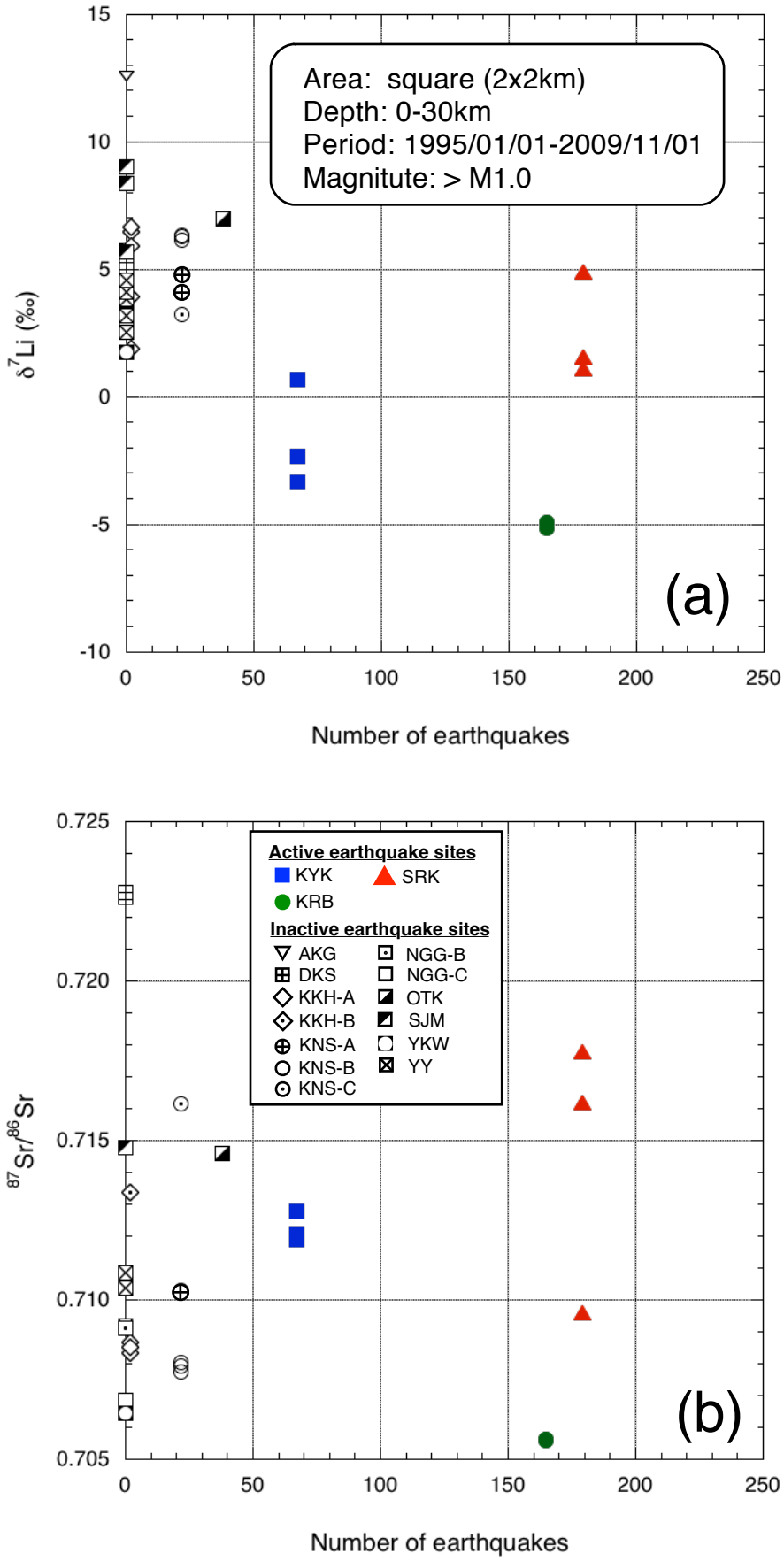

Figure 3 / Nishio et al.

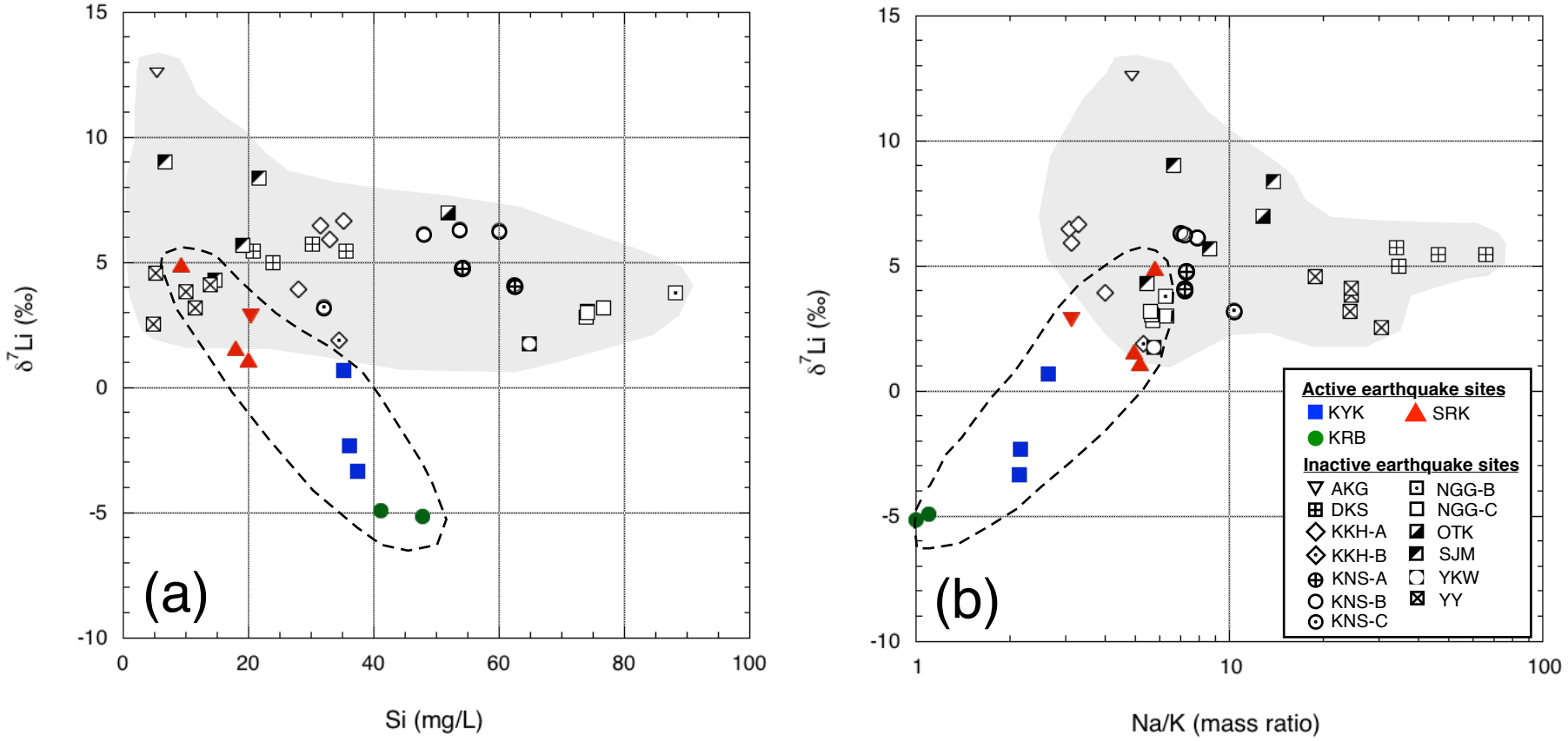

Figure 4 / Nishio et al.

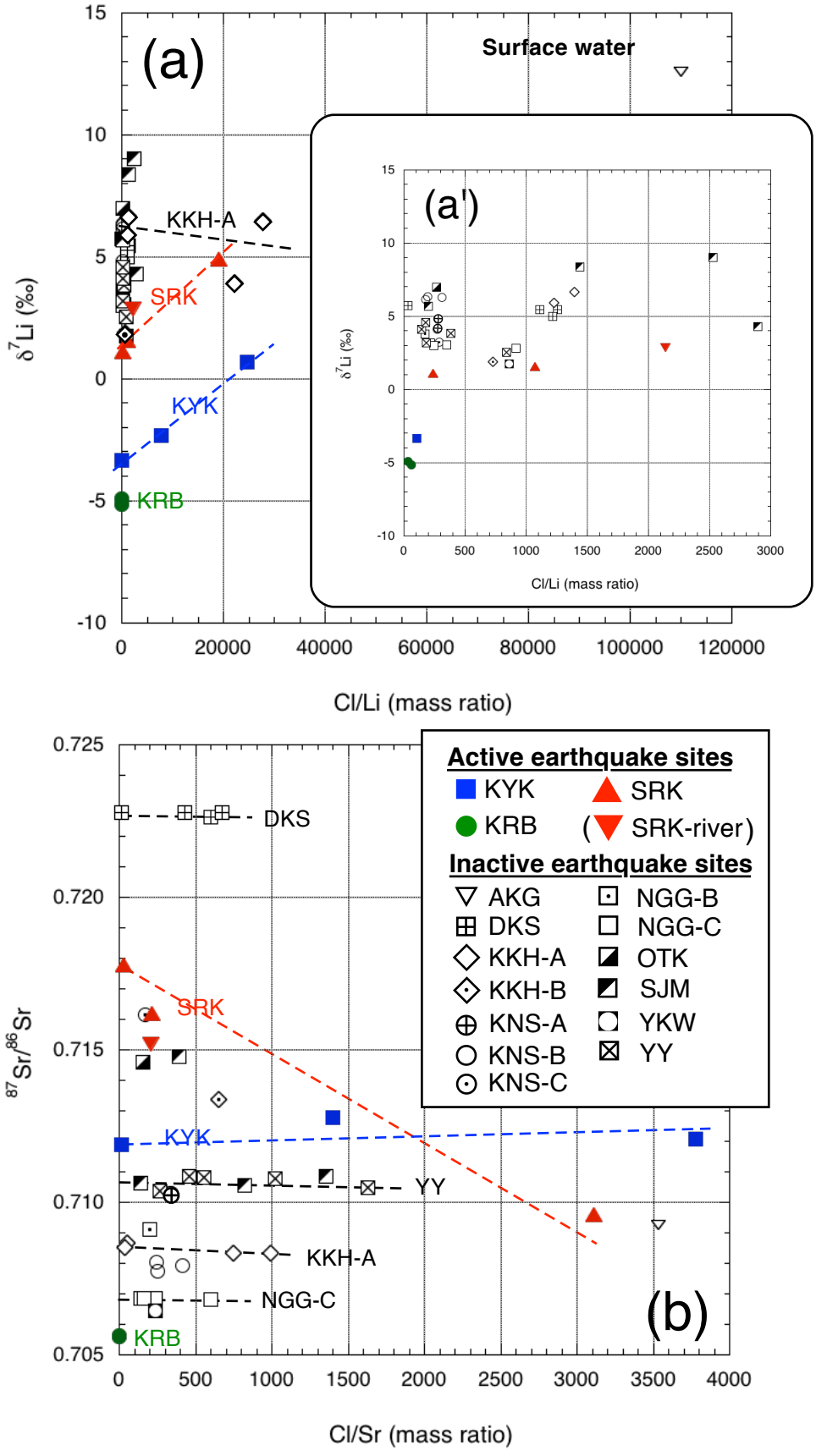

Figure 5 / Nishio et al.

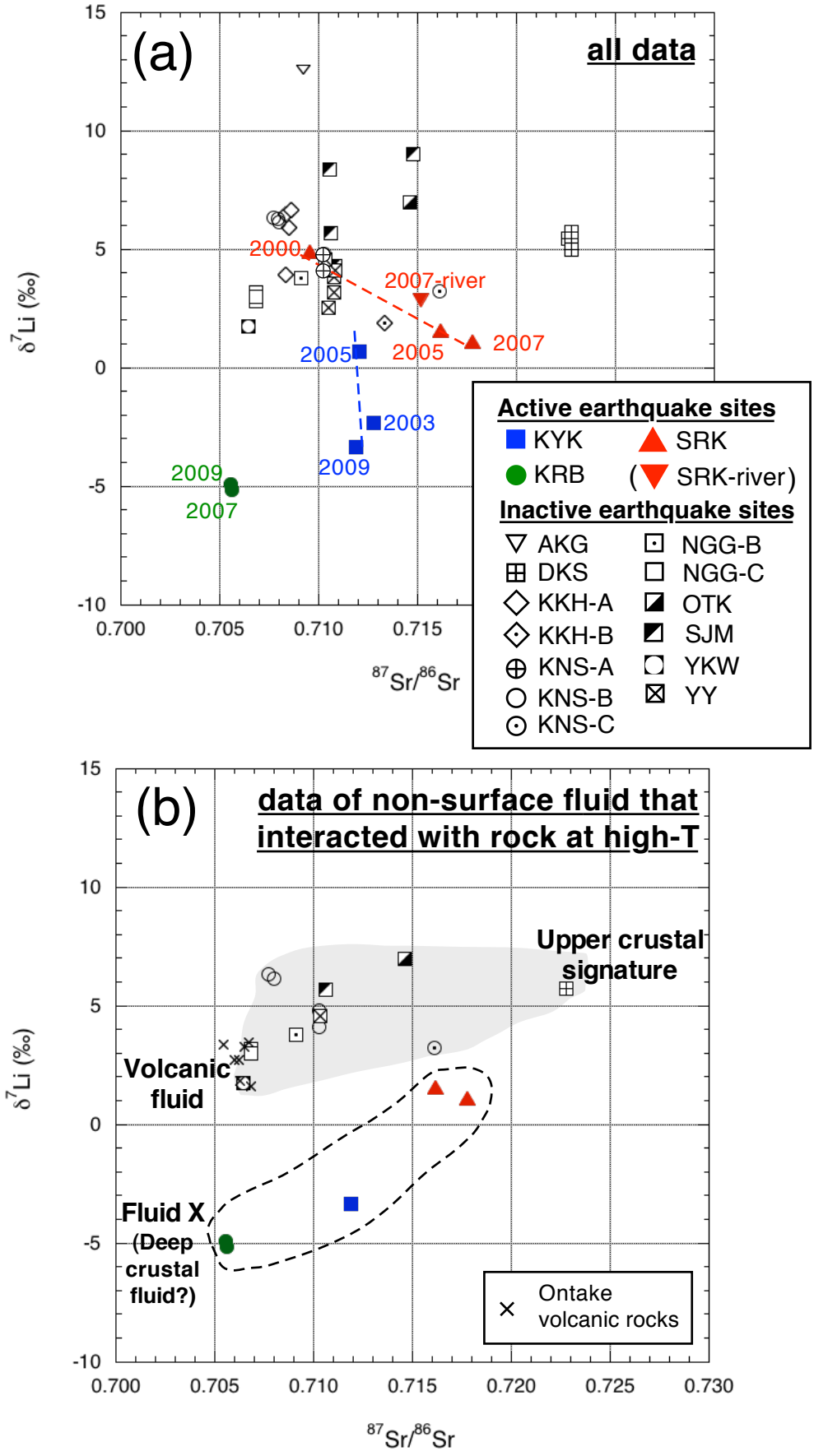

Figure 6 / Nishio et al.

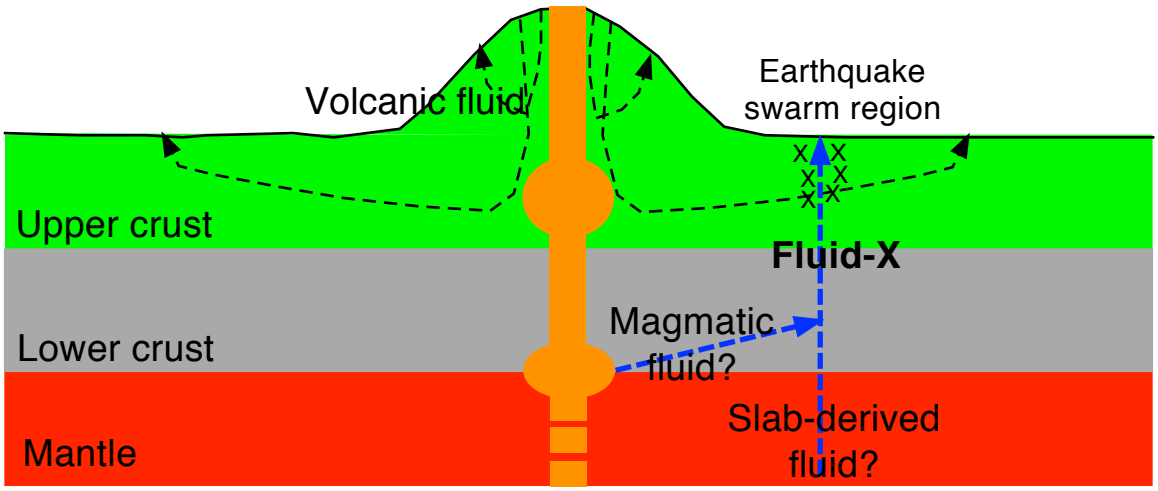

Figure 7 / Nishio et al.